Flow induced by a randomly vibrating boundary

By DMITRI VOLFSON[1] AND JORGE VIÑALS[1,2]

[1]Supercomputer Computations Research Institute, Florida State University, Tallahassee, Florida 32306-4130, USA
[2] Department of Chemical Engineering, FAMU-FSU College of Engineering, Tallahassee, Florida 31310-6046, USA

We study the flow induced by random vibration of a solid boundary in an otherwise quiescent fluid. The analysis is motivated by experiments conducted under the low level and random effective acceleration field that is typical of a microgravity environment. When the boundary is planar and is being vibrated along its own plane, the variance of the velocity field decays as a power law of distance away from the boundary. If a low frequency cut-off is introduced in the power spectrum of the boundary velocity, the variance decays exponentially for distances larger than a Stokes layer thickness based on the cut-off frequency. Vibration of a gently curved boundary results in steady streaming in the ensemble average of the tangential velocity. Its amplitude diverges logarithmically with distance away from the boundary, but asymptotes to a constant value instead if a low frequency cut-off is considered. This steady component of the velocity is shown to depend logarithmically on the cut-off frequency. Finally, we consider the case of a periodically modulated solid boundary that is being randomly vibrated. We find steady streaming in the ensemble average of the first order velocity, with flow extending up to a characteristic distance of the order of the boundary wavelength. The structure of the flow in the vicinity of the boundary depends strongly on the correlation time of the boundary velocity.

1. Introduction

This paper examines the formation and separation of viscous layers in a fluid which is in contact with a solid boundary that is vibrated randomly. The analysis is motivated by the low level and random acceleration field that affects a number of microgravity experiments. We first study the case of a planar boundary to generalize the classical result of Stokes (1851) who considered a boundary vibrated periodically along its own plane. We next consider a slightly curved boundary, and show that steady streaming appears in the ensemble average at first order in the perturbed flow variables. There are several qualitative similarities and differences with the classical result by Schlichting (1979) for the case of periodic vibration. Finally, we address the case of a modulated boundary that is vibrated randomly.

Our study is motivated by the significant levels of residual accelerations (g-jitter) that have been detected during space missions in which microgravity experiments have been conducted (Walter (1987), Nelson (1991), DeLombard *et al.* (1997)). Direct measurement of these residual accelerations has shown that they have a wide frequency spectrum, ranging approximately from $10^{-4}Hz$ to $10^{2}Hz$. Amplitudes range from $10^{-6}g_E$ at the

lowest end of the frequency spectrum, and increase roughly linearly for high frequencies, reaching values of $10^{-4}g_E - 10^{-3}g_E$ at frequencies of around $10Hz$ (g_E is the intensity of the gravitational field on the Earth's surface). Despite the efforts of a number of researchers over the last decade, there remain areas of uncertainty about the potential effect of such a residual acceleration field on typical microgravity fluid experiments, especially in quantitative terms. A better understanding of the response of a fluid to such disturbances would enable improved experiment design to minimize or compensate for their influence. In addition, it would also be useful to have error estimates of quantities measured in the presence of residual accelerations, including whenever possible some methodology for extrapolation to ideal zero gravity.

The formation of viscous layers around solid boundaries when the flow amplitude has a random component has not been addressed yet despite its potential relevance for a number of microgravity experiments. Among them we mention the dynamics of colloidal suspensions, coarsening studies of solid-liquid mixtures in which purely diffusive controlled transport is desired, or the interaction between the viscous layer produced by bulk flow of random amplitude and the morphological instability of a crystal-melt interface. Our study represents the first step in this direction, and focuses on simple geometries in order to elucidate those salient features of the flow that arise from the random nature of the vibration.

Previous theoretical work on the influence of g-jitter on fluid flow ranges from order of magnitude estimates to detailed numerical calculations. For example, the order of magnitude of the contributions to fluid flow from the residual acceleration field may be estimated from the length and time scales of a particular experiment, and the values of the relevant set of dimensionless numbers (Alexander (1990)). Such studies are of interest as a first approximation, but are not very accurate. Other studies have modeled the residual acceleration field by some simple analytic function in which the acceleration is typically decomposed into steady and time dependent components, the latter being periodic in time (Gershuni & Zhukhovitskii (1976), Kamotani *et al.* (1981), Alexander *et al.* (1991), Farooq & Homsy (1994), Grassia & Homsy (1998*a*), Grassia & Homsy (1998*b*), Gershuni & Lyubimov (1998)). A few studies have also addressed the consequences of isolated pulses of short duration (Alexander *et al.* (1997)).

Zhang *et al.* (1993) and Thomson *et al.* (1997) adopted a statistical description of the residual acceleration field onboard spacecraft, and modeled the acceleration time series as a stochastic process in time. The main premise of this approach is that a statistical description is necessary in those cases in which the characteristic time scales of the physical process under investigation are long compared with the correlation time of g-jitter, τ (the acceleration amplitudes and orientations at two different times are statistically independent if separated by an interval larger than τ). Progress has been achieved through the consideration of a specific stochastic model according to which each Cartesian component of the residual acceleration field $\vec{g}(t)$ is modeled as a narrow band noise. This noise is a Gaussian process defined by three independent parameters: its intensity $\langle g^2 \rangle$, a dominant angular frequency Ω, and a characteristic spectral width τ^{-1}. Each realization of narrow band noise can be viewed as a temporal sequence of periodic functions of angular frequency Ω with amplitude and phase that remain constant only for a finite amount of time (τ on average). At random intervals, new values of the amplitude and phase are drawn from prescribed distributions. This model is based on the following mechanism underlying the residual acceleration field: one particular natural frequency of vibration of the spacecraft structure (Ω) is excited by some mechanical disturbance inside the spacecraft, the excitation being of random amplitude and taking place at a sequence of unknown (and essentially random) instants of time.

Narrow band noise has been shown to describe reasonably well many of the features of g-jitter time series measured onboard Space Shuttle by Thomson *et al.* (1997). Actual *g*-jitter data collected during the SL-J mission were analyzed, and a time series of roughly six hours was studied in detail. A scaling analysis revealed the existence of both deterministic and stochastic components in the time series. The deterministic contribution appeared at a frequency of 17 Hz, with an amplitude $\langle g^2 \rangle^{1/2} = 3.56 \times 10^{-4} g_E$. Stochastic components included two well defined spectral features with a finite correlation time; one at 22 Hz with $\langle g^2 \rangle^{1/2} = 3.06 \times 10^{-4} g_E$ and $\tau = 1.09$ s, and one at 44 Hz with $\langle g^2 \rangle^{1/2} = 5.20 \times 10^{-4} g_E$ and $\tau = 0.91$ s. White noise background is also present in the series with an intensity $D = 8.61 \times 10^{-4} \mathrm{cm}^2/\mathrm{s}^3$.

A further theoretical advantage of narrow band noise is that it provides a convenient way of interpolating between monochromatic noise (akin to studies involving a deterministic and periodic gravitational field), and white noise (in which no frequency component is preferred). In the limit $\tau \to 0$ with $D = \langle g^2 \rangle \tau$ finite, narrow band noise reduces to white noise of intensity D; whereas, for $\tau \to \infty$ with $\langle g^2 \rangle$ finite, monochromatic noise is recovered.

We discuss in this paper the flow induced in an otherwise quiescent fluid by the random vibration of a solid boundary. The velocity of the boundary $u_0(t)$ is assumed prescribed, and modeled as a narrow band stochastic process. First, we consider an infinite planar boundary that is being vibrated along its own plane to generalize the classical problem studied by Stokes (1851). In the monochromatic limit, the variance of the velocity field decays exponentially away from the wall, with a characteristic decay length given by the Stokes layer thickness $\delta_s = (2\nu/\Omega)^{1/2}$, where ν is the kinematic viscosity of the fluid, and Ω is the angular frequency of vibration of the boundary. Since the equations governing the flow are linear, we are able to obtain an analytic solution describing transient layer formation in the stochastic case, but only in the neighborhood of the white and monochromatic noise limits. We then show that for any finite correlation time the stationary variance of the tangential velocity asymptotically decays as the inverse squared distance from the wall, in contrast with the exponential decay in the deterministic case. This asymptotic behavior originates from the low frequency range of the power spectrum of the boundary velocity. The crossover from power law to exponential decay is explicitly computed by introducing a low frequency cut-off in the power spectrum.

We next investigate two additional geometries in which the equations governing fluid flow are not linear, and show that several of the generic features obtained for the case of a planar boundary still hold. In the first case, we generalize the analysis of Schlichting (1979) concerning secondary steady streaming. He found that the oscillatory motion of the boundary induces a steady secondary flow outside of the viscous boundary layer even when the velocity of the boundary averages to zero. If the thickness of the Stokes layer, δ_s, and the amplitude of oscillation, a, are small compared with a characteristic length scale of the boundary L ($\delta_s \ll L$, $a \ll L$), then the generation of secondary steady streaming may be described as follows. Vibration of the rigid boundary gives rise to an oscillatory and nonuniform motion of the fluid. The flow is potential in the bulk, and rotational in the boundary layer because of no-slip conditions on the boundary. The bulk flow applies pressure at the outer edge of boundary layer, which does not vary across the layer. The non uniformity of the flow leads to vorticity convection in the boundary layer through nonlinear terms. Both convection and the applied pressure drive vorticity diffusion, and thus induce secondary steady motion which does not vanish outside of the boundary layer. In the simplest case in which the far field velocity is a standing wave

$U(x,t) = U(x)\cos(\Omega t)$, the tangential component of the secondary steady velocity is,

$$u^{(s)} = -\frac{3}{4\Omega}U\frac{\mathrm{d}U}{\mathrm{d}x}, \tag{1.1}$$

where x is a curvilinear coordinate along the boundary. In fact, Eq. (1.1) serves as the boundary condition for the stationary part of the flow in the bulk. Similar conclusions have been later reached by Batchelor (1967) who studied sinusoidal oscillations of nonuniform phase, and by Gershuni & Lyubimov (1998) who studied monochromatic oscillations of a general form.

The second geometry that we address is the so called wavy wall (Lyne (1971)). The deterministic limit in which a wavy boundary is being periodically vibrated has been studied by a number of authors, mainly to address the interaction between the flow above the sea bed and ripple patterns on it (Lyne (1971), Kaneko & Honjii (1979), Vittori (1989), Blondeaux & Vittori (1994) and references therein). Lyne (1971) deduced the existence of steady streaming in the limit in which the amplitude of the wall deviation from planarity is small compared with the thickness of the Stokes layer. He introduced a conformal transformation and obtained an explicit solution in the limit of small kRe, where k is the wavenumber of the wall profile scaled by the thickness of the Stokes layer, and Re is the Reynolds number. The detailed structure of the secondary flow depends on the ratio between the wavelength of the boundary profile and the thickness of the Stokes layer.

In Sections 3 and 4, we discuss how the results for these two geometries generalize to the case of stochastic vibration. Section 3 addresses the flow created by a gently curved solid boundary that is being vibrated randomly. The perturbation parameter that we use is the ratio between the amplitude of vibration and the characteristic inverse curvature of the wall. The ensemble average of the stream function is not zero, and hence there exists stationary streaming in the stochastic case as well. The average velocity diverges logarithmically away from the boundary because of the low frequency range of the power spectrum. We again introduce a low frequency cut-off ω_c in the spectrum, and study the dependence of the stationary streaming on the cut-off frequency. We compute the stationary tangential velocity as a function of $\omega_c \ll 1$ and arbitrary β, and find a weak (logarithmic) singularity as $\omega_c \to 0$.

Section 4 discusses the formation of a boundary layer around a wavy boundary that is vibrated randomly. Positive and negative vorticity production in adjacent regions of the boundary introduces a natural decay length in the solution, thus leading to exponential decay of the flow away from the boundary, even in the absence of a low frequency cut-off in the power spectrum of the boundary velocity. Steady streaming is found at second order comprising two or four recirculating cells per period of the boundary profile. The number of cells depends on the scaled correlation time $\Omega\tau$.

2. Randomly vibrating planar boundary

We first examine the case of a planar boundary that is being vibrated along its own plane. In this case the governing equations are considerably simpler then in the more general geometries discussed in Sections 3 and 4. In particular, the Navier-Stokes equation is linear, fact that allows a complete solution of the flow. Nevertheless, this simple solution still exhibits several of the qualitative features that are present in the case of random forcing by a curved boundary, namely asymptotic power law decay of the velocity field away from the boundary, and sensitive dependence on the low frequency range of the power spectrum of the boundary velocity.

Consider an infinite solid boundary located at $z = 0$, and an incompressible fluid that occupies the region $z > 0$. The Navier-Stokes equation, and boundary conditions are,

$$\partial_t u = \nu \partial_z^2 u, \tag{2.1}$$

$$u(0, t) = u_0(t), \quad u(\infty, t) < \infty, \tag{2.2}$$

where z is the coordinate normal to the boundary, $u(z, t)$ is the x component of the velocity, and $u_0(t)$ is the prescribed velocity of the boundary. The solution for harmonic vibration $u_0(t) = u_0\cos(\Omega t)$ was given by Stokes (1851). It is a transversal wave that propagates into the bulk fluid with an exponentially decaying amplitude,

$$u(z, t) = u_0 e^{-z/\delta_s}\cos(\Omega t - z/\delta_s), \tag{2.3}$$

where $\delta_s = (2\nu/\Omega)^{1/2}$ is the Stokes layer thickness.

2.1. *Narrow band noise*

As discussed in the introduction, the main topic of this paper is to examine how the nature of the bulk flow changes when the boundary velocity $u_0(t)$ is a random process. Specifically, we consider a Gaussian process defined by

$$\langle u_0(t) \rangle = 0, \quad \langle u_0(t)u_0(t') \rangle = \langle u_0{}^2 \rangle e^{-|t-t'|/\tau}\cos\Omega(t - t'). \tag{2.4}$$

This process is known as narrow band noise (Stratonovich (1967)). It is defined by three independent parameters: its variance $\langle u_0^2 \rangle$, its dominant angular frequency Ω, and the correlation time τ. Each realization of this random process can be viewed as a sequence periodic functions of frequency Ω, with amplitude and phase that remain constant for a time interval τ on average. White noise is recovered when $\Omega\tau \to 0$ while $D = \langle u_0{}^2 \rangle \tau$ remains finite, whereas the monochromatic noise limit corresponds to $\Omega\tau \to \infty$, with $\langle u_0{}^2 \rangle$ finite. Monochromatic noise is akin to a single frequency periodic signal of the same frequency, but with randomly drawn amplitude and phase. The relationship between the two can be illustrated by considering a deterministic function $x(t) = x_0\cos(\Omega t)$ and defining the temporal average as,

$$\langle x(t)x(t') \rangle = \lim_{T\to\infty} \frac{1}{T} \int_0^T dt\, x(t)x(t') = \frac{x_0^2}{2}\cos(\Omega(t - t')). \tag{2.5}$$

This average coincides with the ensemble average of the noise when $\langle u_0^2 \rangle = x_0^2/2$. The power spectrum corresponding to the correlation function (2.4) is

$$P(\omega) = \frac{\langle u_0^2 \rangle}{2\pi} \left[\frac{\tau}{1 + \tau^2(\omega - \Omega)^2} + \frac{\tau}{1 + \tau^2(\omega + \Omega)^2} \right]. \tag{2.6}$$

We will also use the spectral density of the process $u_0(t)$,

$$\hat{u}_0(\omega) = \frac{1}{2\pi} \int_{-\infty}^{\infty} dt\, u_0(t)e^{-i\omega t}, \tag{2.7}$$

so that its ensemble average and correlation function are respectively given by

$$\langle \hat{u}_0(\omega) \rangle = 0, \quad \langle \hat{u}_0(\omega)\hat{u}_0^*(\omega') \rangle = \delta(\omega - \omega')P(\omega). \tag{2.8a, b}$$

We will often use dimensionless variables in which $\langle u_0^2 \rangle /\Omega$ is the scale of $P(\omega)$, and Ω is the angular frequency scale. In dimensionless form,

$$P(\omega, \beta) = \frac{1}{2\pi} \left[\frac{\beta}{1 + \beta^2(\omega - 1)^2} + \frac{\beta}{1 + \beta^2(\omega + 1)^2} \right], \tag{2.9}$$

where $\beta = \Omega\tau$. We have $\int_{-\infty}^{\infty} d\omega P(\omega, \beta) = 1$, independent of β, and also $\lim_{\beta\to\infty} P(\omega) = [\delta(\omega - 1) + \delta(\omega + 1)]/2$. Note that the power spectrum does not vanish at small frequencies. Instead, $P(0, \beta) = \beta/(\pi(1 + \beta^2))$, which for large and small β behaves as $P(0, \beta) \sim 1/(\pi\beta)$ and $P(0, \beta) \sim \beta/\pi$ respectively. We will discuss separately the effect of this low frequency contribution on the results presented in the remainder of the paper.

2.2. *Transient layer formation*

In the two limiting cases of white and monochromatic noise, it is possible to find an analytic solution for the transient flow starting from an initially quiescent fluid. The solution can be found, for example, by introducing the retarded, infinite space Green's function corresponding to equation (2.1), with boundary conditions (2.2),

$$G(z, t|z', t') = \frac{1}{(4\pi\nu(t - t'))^{1/2}} \left[e^{-(z-z')^2/4\nu(t-t')} - e^{-(z+z')^2/4\nu(t-t')} \right], \quad t > t', \quad (2.10)$$

and $G(z, t|z', t') = 0$ for $t < t'$. If the fluid is initially quiescent, $u(z, 0) = 0$, we find

$$u(z, t) = \nu \int_0^t dt' \, u_0(t') \left(\partial_{z'} G \right)_{z'=0}, \qquad (2.11)$$

with

$$\left(\partial_{z'} G \right)_{z'=0} = \frac{z}{[4\pi\nu^3(t - t')^3]^{1/2}} \, e^{-z^2/4\nu(t-t')}. \qquad (2.12)$$

Equations (2.11-2.12) determine the transient behavior for any given $u_0(t)$.

If $u_0(t)$ is a Gaussian, white noise process, the ensemble average of Eq.(2.11) yields $\langle u(z, t) \rangle = 0$. The corresponding equation for the variance reads

$$\left\langle u^2(z, t) \right\rangle = 2D\nu^2 \int_0^t dt' \, [(\partial_{z'} G)_{z'=0}]^2 = \frac{2D\nu}{\pi z^2} \left(1 + \frac{z^2}{2\nu t} \right) e^{-z^2/2\nu t}. \qquad (2.13)$$

The variance of the induced fluid velocity propagates into the fluid diffusively. Saturation occurs for $t \gg z^2/2\nu$, at which point the variance does not decay exponentially far away from the wall, but rather as a power law.

$$\left\langle u^2(z, \infty) \right\rangle = \frac{2D\nu}{\pi z^2}. \qquad (2.14)$$

Ascertaining whether random vibration can induce flows far away from the boundary in more general geometries is one of the main motivations for this paper.

Consider now the opposite limit of monochromatic noise with correlation function

$$\langle u_0(t) u_0(t') \rangle = \left\langle u_0^2 \right\rangle \cos \left[\Omega(t - t') \right]. \qquad (2.15)$$

Now using Eqs. (2.11) and (2.15) we find, (Carslaw & Jaeger (1959)),

$$\frac{\langle u^2(z, t) \rangle}{2 \langle u_0^2 \rangle} = \frac{2}{\pi} \int_\kappa^\infty d\sigma \, e^{-\sigma^2} \int_\kappa^\infty d\mu \, e^{-\mu^2} \cos \left[\frac{z^2}{2\delta_s^2} \left(\frac{1}{\mu^2} - \frac{1}{\sigma^2} \right) \right], \qquad (2.16)$$

with $\kappa = z/(4\nu t)^{1/2}$. A closed form solution can only be obtained for long times. We find,

$$\frac{\langle u^2(z, t) \rangle}{2 \langle u_0^2 \rangle} = \frac{e^{-2z/\delta_s}}{2} + \frac{2\kappa^3 \delta_s^2}{\pi^{1/2} z^2} e^{-z/\delta_s} \sin(\Omega t - z/\delta_s) + \mathcal{O}(\kappa^5(t)). \qquad (2.17)$$

At long times, the variance propagates into the bulk with phase velocity $(2\nu\Omega)^{1/2}$, while its amplitude decays exponentially in space over the scale of the Stokes layer, and as

$t^{-3/2}$ in time. In summary, the flow created by the vibration of the boundary propagates diffusively for white noise ($z^2 \propto 2\nu t$), and as a power law ($z^2 \propto \pi\nu\Omega^2 t^3$) in the monochromatic limit.

2.3. *Stationary variance for narrow band noise*

We have been unable to obtain a closed analytic solution for the transient evolution of the variance $\langle u(z,t)^2 \rangle$ when the vibration of the boundary is given by a general narrow band process. It is possible, however, to obtain the stationary variance of the velocity. Equation (2.1) can be rewritten in Fourier space as

$$i\omega \hat{u}(z,\omega) = \nu \partial_z^2 \hat{u}(z,\omega) \tag{2.18}$$

with

$$u(z,t) = \int_{-\infty}^{\infty} d\omega \, \hat{u}(z,\omega) e^{i\omega t}, \tag{2.19}$$

The boundary conditions are, $\hat{u}(0,\omega) = \hat{u}_0(\omega)$, and $\hat{u}(z,\omega) < \infty$ at $z \to \infty$. The solution of Eq. (2.18) with these boundary conditions is

$$\hat{u}(z,\omega) = e^{-\alpha z} \hat{u}_0(\omega), \quad \alpha = (1 + i\,\text{sign}(\omega))(\omega/2\nu)^{1/2} \tag{2.20}$$

We next choose $1/\Omega$ as the time scale, and δ_s as the length scale, and after some straightforward algebra we find,

$$\frac{\langle u^2(z,\beta) \rangle}{2\langle u_0^2 \rangle} = I(z,\beta) = \int_0^{\infty} d\omega P(\omega,\beta) e^{-z\omega^{1/2}}. \tag{2.21}$$

We have also used the fact that the power spectrum (2.9) is even in frequency.

We next analyze the asymptotic dependence of $I(z,\beta)$ at large z. In this limit, $I(z,\beta)$ mainly depends on the low frequency region of the power spectrum; higher frequencies are suppressed by the exponential factor. By using Watson's lemma (Nayfeh (1981)), we find,

$$I(z,\beta) = \frac{2\beta}{\pi(1+\beta^2)} \frac{1}{z^2} + \frac{240\beta^3(3\beta^2-1)}{\pi(1+\beta^2)^3} \frac{1}{z^6} + \mathcal{O}(z^{-10}). \tag{2.22}$$

This asymptotic form at large z is valid for all β. In particular, the dominant behavior for small and large β is

$$I(z,\beta) \sim \frac{2\beta}{\pi} \frac{1}{z^2}, \quad I(z,\beta) \sim \frac{2}{\pi\beta} \frac{1}{z^2},$$

respectively. Hence we recover the power law decay of Eq. (2.14).

We can also find the asymptotic behavior at large β that is uniformly valid in z,

$$I(z,\beta) = \frac{e^{-z}}{2} - \frac{z}{2\pi\beta} \left(\text{Ci}(z)\sin(z) - \text{Si}(z)\cos(z) - \frac{1}{2}(e^{-z}\text{Ei}(z) - e^z\text{Ei}(-z)) \right) + \mathcal{O}(\beta^{-3}), \tag{2.23}$$

where Ci and Si denote the integral sine and cosine functions, and Ei stands for the exponential integral function (Gradshteyn & Ryzhik (1980)). For $z \lesssim 1$, the variance decreases exponentially. At larger z, the exponential terms in (2.23) become small, so that the remaining asymptotic dependence for large z is given by Eq. (2.22). The quantity $I(z,\beta) z^2$ computed both from (2.21) and the uniform expansion (2.23) is presented in Fig.1. For fixed β, $I(z,\beta)$ asymptotes to $2\beta/\pi(1+\beta^2)$ outside of Stokes layer. This value is the coefficient of the leading term in the asymptotic expansion (2.22). The expansion (2.23) is a good approximation even for moderate values of β.

To summarize, the variance of the velocity field does not decay exponentially away from the wall for finite β, but rather as the inverse squared distance. The crossover length separating exponential and power law decay increases with increasing β.

2.4. *Low frequency cut-off in the power spectrum*

The coefficient of the leading term in (2.22) is in fact twice the value of $P(0, \beta) = \beta/\pi(1 + \beta^2)$. The algebraic decay of $\langle u_0^2(z,t) \rangle$ follows from the diffusive nature of Eq. (2.1), and a non vanishing value of $P(\omega, \beta)$ as $\beta \to 0$. Before we analyze in Sections 3 and 4 how this behavior is modified by nonlinearities in the governing equations, we explicitly address here the consequences of a low frequency cut-off in the power spectrum. Of course, there always exists in practice a low frequency cut-off because of limited observation time. Furthermore, the low frequency range of the power spectrum of the residual acceleration field in microgravity ($\Omega/2\pi < 10^{-3}$Hz) is fairly difficult to measure reliably. We therefore introduce an effective cut-off frequency in the power spectrum, $\omega_c \ll 1$, and study the dependence of $\langle u_0^2(z,t) \rangle$ on ω_c. The stationary value of variance of the velocity is now given by,

$$\frac{\langle u^2(z, \beta, \omega_c) \rangle}{2 \langle u_0^2 \rangle} = I_c(z, \beta, \omega_c) = \int_{\omega_c}^{\infty} d\omega P(\omega, \beta) e^{-z\omega^{1/2}}. \qquad (2.24)$$

By using Watson's lemma, we find for large z,

$$I_c(z, \beta, \omega_c) = \frac{2\beta e^{-z\omega_c^{1/2}}}{\pi(1 + \beta^2)} \left(\frac{1}{z^2} + \frac{\omega_c^{1/2}}{z} + \text{h.o.t.} \right), \qquad (2.25)$$

where h.o.t. stands for terms which are of higher order than terms retained under the assumption that both $1/z$ and $\omega_c^{1/2}$ are small but independent. For $z \gg 1$, but $z\omega_c^{1/2} \ll 1$ the dominant term in (2.25) is

$$I_c(z, \beta, \omega_c) \sim \frac{2\beta}{\pi(1 + \beta^2)} \frac{1}{z^2}, \quad z\omega_c^{1/2} << 1. \qquad (2.26)$$

On the other hand, if $z\omega_c^{1/2} \geqslant 1$, the leading order term is now a function of $\zeta = z\omega_c^{1/2}$

$$I_c(z, \beta, \omega_c) \sim \frac{2\beta\omega_c e^{-\zeta}}{\pi(1 + \beta^2)} \left(\frac{1}{2\zeta} + \frac{1}{\zeta^2} \right), \quad \zeta \geqslant 1 \qquad (2.27)$$

Equations (2.26) and (2.27) show that at distances that are large compared with the thickness of the Stokes layer based on the dominant frequency Ω, $\langle u^2(z,t) \rangle$ decays algebraically with z. There exists, however, a length scale $z\omega_c^{1/2}$ beyond which the decay is exponential. This new characteristic length scale is the thickness of the Stokes layer based on the cut-off frequency. This conclusion appears natural given the principle of superposition for the linear differential equation (2.1).

3. Streaming due to random vibration

Next we investigate to what extent the results of Section 2 hold in configurations in which the governing equations are not linear. We examine in this section the flow induced by a gently curved solid boundary that is being randomly vibrated. The boundary velocity is assumed to be described by a narrow band stochastic process, and hence our results will reduce to Schlichting's in the limit of infinite correlation time. However, for finite values of β the results are qualitatively different. The mechanism of secondary steady streaming generation described in the introduction is no longer valid because there is no

boundary layer solution at zeroth order. Vorticity produced at the vibrating boundary penetrates into the bulk fluid, at least perturbatively for small curvature. This results in a logarithmic divergence of the ensemble average of the first order velocity with distance away from the wall. A cut-off analysis is also presented, and similarly to that of Section 2.4, it reveals the existence of an effective boundary layer of thickness based on the cut-off frequency. We then find an expression analogous to Eq. (1.1) as a function of β and ω_c.

Define the following dimensionless quantities,

$$\left.\begin{array}{c} z = \tilde{z}[(\nu/\Omega)^{1/2}], \quad x = \tilde{x}[L], \quad t = \tilde{t}[\Omega^{-1}], \quad \psi = \tilde{\psi}[(2\left\langle u_0^2\right\rangle \nu/\Omega)^{1/2}], \\[2mm] \epsilon = (2\left\langle u_0^2\right\rangle)^{1/2}/\Omega L, \quad Re_p = 2\left\langle u_0^2\right\rangle/\Omega\nu, \quad \tilde{\Delta} = \partial_{\tilde{z}}^2 + \epsilon^2/Re_p\partial_{\tilde{x}}^2 \end{array}\right\} \tag{3.1}$$

Assume now that the characteristic scale of the boundary L is large so that ϵ is a small quantity. If the Reynolds number Re_p is assumed to remain finite, both conditions imply $\nu/\Omega L^2 \ll 1$. We next write the governing equations and boundary conditions in the frame of reference co-moving with the solid boundary and obtain for a two dimensional geometry (tildes are omitted),

$$\partial_t\Delta\psi + \epsilon\frac{\partial(\psi, \Delta\psi)}{\partial(z, x)} = \Delta^2\psi \tag{3.2}$$

$$\psi = 0, \quad \partial_z\psi = 0 \quad \text{at} \quad y = 0, \tag{3.3a, b}$$

$$\partial_z\psi = 2^{-1/2}U(x)u_0(t) \quad \text{at} \quad z = \infty, \tag{3.4}$$

where x, z are the tangential and normal coordinates along the boundary, and ψ is the stream function $\boldsymbol{u} = (\partial_z\psi, -\partial_x\psi)$. We have also used the notation $\partial(a, b)/\partial(z, x) = (\partial_z a)(\partial_x b) - (\partial_x a)(\partial_z b)$ for the nonlinear term. The far field boundary condition is a nonuniform and random velocity field, of the order of $\left\langle u_0^2\right\rangle^{1/2}$, with a spatially nonuniform amplitude $U(x)$, and a stochastic modulation $u_0(t)$ which is a Gaussian stochastic process with zero mean, and narrow band power spectrum. We first expand the stream function as a power series of ϵ, $\psi = \psi_0 + \epsilon\psi_1 + \dots$ and solve (3.2) order by order. At order ϵ^0 we obtain the following equation,

$$(\partial_t\partial_z^2 - \partial_z^4)\psi_0 = 0 \tag{3.5}$$

with boundary conditions,

$$\psi_0 = 0, \quad \partial_z\psi = 0 \quad \text{at} \quad z = 0, \tag{3.6a, b}$$

$$\partial_z\psi = 2^{-1/2}U(x)u_0(t) \quad \text{at} \quad z = \infty. \tag{3.7}$$

At this order, the equations effectively describe the flow induced above a planar boundary with a far field velocity boundary condition that is not uniform. The solution can be found by Fourier transformation. We define,

$$\psi_0(x, z, t) = \int_{-\infty}^{\infty} d\omega\, \hat{\psi}_0(x, z, \omega)e^{i\omega t}. \tag{3.8}$$

The transformed Eq. (3.5) and the transformed boundary conditions (3.6) allow separation of variables. We define,

$$\hat{\psi}_0(x, z, \omega) = 2^{-1/2}U(x)\hat{u}_0(\omega)\hat{\zeta}_0(z, \omega),$$

so that Eq. (3.5) leads to,

$$(i\omega\partial_z^2 - \partial_z^4)\hat{\zeta}_0 = 0, \tag{3.9}$$

with boundary conditions $\hat{\zeta}_0 = 0$, $\partial_z\hat{\zeta}_0 = 0$, at $z = 0$ and $\partial_z\hat{\zeta}_0 = 1$ at $z = \infty$. The solution is,

$$\hat{\zeta}_0(z,\omega) = -1/\alpha + z + 1/\alpha e^{-\alpha z}, \quad \alpha(\omega) = (1 + i\,\mathrm{sign}(\omega))(|\omega|/2)^{1/2}). \tag{3.10}$$

At order ϵ we find,

$$(\partial_t\partial_z^2 - \partial_z^4)\psi_1 = \partial_x\psi_0\partial_z^3\psi_0 - \partial_z\psi_0\partial_x\partial_z^2\psi_0 \tag{3.11}$$

with boundary conditions $\psi_1 = 0$, $\partial_z\psi_1 = 0$ at $y = 0$. The remaining boundary condition for ψ_1 needs to be discussed separately. Consider first the classical deterministic limit which can be formally obtained by setting $\beta = \infty$. Then, the right hand side of Eq. (3.11) involves stationary terms (of zero frequency), and sinusoidal terms with twice the frequency of the far field flow. Since the equation is linear, the solution ψ_1 has exactly the same temporal behavior. In this case, it is known that it is not possible to find a solution for $\partial_z\psi_1$ that vanishes at large z, but only one that simply remains bounded as $z \to \infty$. By analogy, we introduce a similar requirement in the stochastic case of $\beta < \infty$. Since the zeroth order stream function diverges linearly, this condition simply amounts to requiring that the expansion in powers of ϵ remains consistent.

We now take the ensemble average of Eq. (3.11), and consider the long time stationary limit of the average ($\psi_1^{(s)} = \lim_{t\to\infty}\langle\psi_1\rangle$), to find,

$$\partial_z^4\psi_1^{(s)} = \left\langle\partial_z\psi_0\partial_x\partial_z^2\psi_0 - \partial_x\psi_0\partial_z^3\psi_0\right\rangle. \tag{3.12}$$

The right hand side of this equation can be integrated from infinity to z. We obtain,

$$\partial_z^3\psi_1^{(s)} = \frac{U}{2}\frac{\mathrm{d}U}{\mathrm{d}x}F(z,\beta), \tag{3.13}$$

where

$$F(z,\beta) = \int_0^\infty \mathrm{d}\omega P(\omega,\beta)Q(\omega,z),$$

and

$$Q(\omega,z) = (-2 + 2\hat{\zeta}_0\partial_z\hat{\zeta}_0^* - \hat{\zeta}_0\partial_z^2\hat{\zeta}_0^* - \hat{\zeta}_0^*\partial_z^2\hat{\zeta}_0).$$

The power spectrum $P(\omega,\beta)$ is defined in Eq. (2.9). The constant that appears in the expression for $Q(\omega,z)$ comes from the pressure gradient imposed at infinity.

We now proceed to solve Eq. (3.13) subject to the boundary conditions $\psi_1^{(s)} = \partial_z\psi_1^{(s)} = 0$ on the solid boundary, and $\partial_z\psi_1^{(s)} < \infty$ as $z \to \infty$. This is a boundary value problem for $\psi_1^{(s)}$. In the limit $\beta \to \infty$, it can be solved analytically, and the result obtained by Schlichting is recovered, namely that the solution may be bounded at infinity simply by setting the homogeneous part of the solution equal to zero to satisfy the principle of minimal singularity (Van Dyke (1964)). Otherwise $\partial_z\psi_1^{(s)}$ is singular a fortiori. Since we cannot find an complete analytic solution for finite β, we proceed as follows. We recast the boundary value problem as an initial value problem, and search for a boundary condition on $\partial_z^2\psi_1^{(s)}$ at $z = 0$ so that the homogeneous part of the solution remains bounded. This boundary condition can be found analytically by integrating (3.13) from 0 to z. We find,

$$\partial_z^2\psi_1^{(s)}(z) - \partial_z^2\psi_1^{(s)}(0) = \frac{U}{2}\frac{\mathrm{d}U}{\mathrm{d}x}\int_0^z \mathrm{d}z'\int_0^\infty \mathrm{d}\omega P(\omega,\beta)Q(\omega,z'),$$

or after changing the order of integration,

$$\partial_z^2\psi_1^{(s)}(z) - \partial_z^2\psi_1^{(s)}(0) = \frac{U}{2}\frac{\mathrm{d}U}{\mathrm{d}x}\int_0^\infty \mathrm{d}\omega P(\omega,\beta)\left[\int_z \mathrm{d}z'Q(\omega,z') - \left(\int_z \mathrm{d}z'Q(\omega,z')\right)_{z=0}\right].$$

The second integral within brackets equals $(1/2\omega)^{1/2}$. In order to avoid a linear divergence of $\partial_z \psi_1^{(s)}(z)$ we equate the constant terms on both sides, thus obtaining the third initial condition

$$\partial_z^2 \psi_1^{(s)}(0, \beta) = U \frac{\mathrm{d}U}{\mathrm{d}x} \frac{2^{1/2}}{4} \int_0^\infty \mathrm{d}\omega\, \omega^{-1/2} P(\omega, \beta) =$$
$$= U \frac{\mathrm{d}U}{\mathrm{d}x} \frac{(2\beta)^{1/2}}{8q} ((2(q - \beta))^{1/2} + (q + 1)^{1/2} + (q - 1)^{1/2}), \qquad (3.14)$$

where $q = (1 + \beta^2)^{1/2}$, and the dependence of initial condition on β is shown explicitly. Equation (3.13) with its original boundary conditions, supplemented with Eq. (3.14) is an initial value problem, which we have solved numerically.

Before presenting the numerical results, we study the asymptotic behavior of the solution for large z which is determined by the asymptotic form of $F(z, \beta)$ at large z. By explicit substitution of the zeroth order solution we find

$$Q(z, \omega) = (-4\cos(Z) - 2Z(\cos(Z) + \sin(Z)) + 2\sin(Z))\mathrm{e}^{-Z} + 2\mathrm{e}^{-2Z}, \qquad (3.15)$$

where $Z = z(\omega/2)^{1/2}$. The leading contribution to $F(z, \beta)$ as $z \to \infty$ originates from the zero frequency limit of $P(\omega, \beta)$. Thus $F(z, \beta) \sim P(0, \beta) \int_0^\infty \mathrm{d}\omega Q(\omega, z)$. The remaining integral may be easily calculated to yield the asymptotic form,

$$F(z, \beta) \sim \frac{6\beta^2}{\pi(1 + \beta^2)} \frac{1}{z^2}. \qquad (3.16)$$

Therefore the stationary mean first order velocity $u_1^{(s)} = \partial_z \psi_1^{(s)}$ has a logarithmic asymptotic form (see Eq. (3.13)). This is to be contrasted with the power law decay of the stationary variance for the case of a randomly vibrating planar boundary.

Finally, we have numerically calculated $\partial_z \psi_1^{(s)}(z)$ for a range of values of β. The results are presented in Fig. 2. Equation (3.13) was integrated numerically with no-slip boundary conditions for $\psi_1^{(s)}$, and Eq. (3.14). The numerical results support our conclusion about the logarithmic divergence of $u_1^{(s)}$ with distance for any finite β. As β increases the stationary mean velocity profile approaches a limiting form that corresponding to the monochromatic limit of $\beta \to \infty$. In this limit we recover the Schlichting result, according to which $\partial_z \psi_1^{(s)}(z)$ asymptotes to a constant value over a distance of the order of the deterministic Stokes layer.

3.1. *Low frequency cut-off in the power spectrum*

In Section 2, we showed that a low frequency cut-off in $P(\omega, \beta)$ led to an exponential decay of the velocity outside an effective boundary layer of thickness determined by the cut-off frequency. We therefore examine here the consequences of a low frequency cut-off on the divergent behavior of the stationary average of the first order stream function. In order to find the asymptotic form of $\partial_z \psi_1^{(s)}$, we first integrate (3.13) twice from $z = 0$ to z. By using the low frequency cut-off defined in Section (2.4), we write,

$$\partial_z \psi_1^{(s)}(z, \beta, \omega_c) = \frac{U}{2} \frac{\mathrm{d}U}{\mathrm{d}x} \left[G_c(z, \beta, \omega_c) - G_c(0, \beta, \omega_c) \right], \qquad (3.17)$$

with,

$$G_c(z, \beta, \omega_c) = \int \mathrm{d}z' \int \mathrm{d}z' F_c(z', \beta, \omega_c),$$

and,

$$F_c(z, \beta, \omega_c) = \int_{\omega_c}^{\infty} \mathrm{d}\omega \, P(\omega, \beta) Q(\omega, z).$$

If we set $\omega_c = 0$ and consider the monochromatic limit of $\beta \to \infty$, we find that $G_c(z, \infty, 0)$ contains an exponential factor that vanishes at $z \sim \mathcal{O}(1)$, and that $G_c(0, \infty, 0) = 3/4$. Therefore the Schlichting result is recovered. An explicit form of $G_c(z, \beta, \omega_c)$ for any β and ω_c can be obtained analytically, but it is far too complicated and we do not quote it here. It has a similar functional dependence as in the cut-off analysis of the planar boundary, and contains exponential terms involving $(-z\omega_c^{1/2})$. We find that $\partial_z \psi_1^{(s)}(\infty, \beta, \omega_c) = -U \mathrm{d}U/2\mathrm{d}x \, G_c(0, \beta, \omega_c)$. For finite but small ω_c, we find,

$$\partial_z \psi_1^{(s)}(\infty, \beta, \omega_c) = -\frac{3}{4} U \frac{\mathrm{d}U}{\mathrm{d}x} \frac{\beta}{\pi(1+\beta^2)} \left(2\beta \arctan(\beta) - \ln\left(\frac{\beta^2 \omega_c^2}{1+\beta^2} \right) \right) + \mathcal{O}(\omega_c^2) \quad (3.18)$$

This asymptotic formula is compared with the numerically computed value of the tangential mean stationary velocity at large distances in Figure 4. Computations were done as described in the previous section, and for different values of $\omega_c \ll 1$ and β. In all cases $\partial_z \psi_1^{(s)}$ reached constant values at large enough z (the numerical value of infinity, z_∞, was chosen so that the change in velocity for $z \geqslant z_\infty$ was less than a prescribed tolerance). We also checked that any change in the boundary condition Eq.(3.14) leads to a linear divergence in the tangential mean stationary velocity, thus confirming the adequacy of this boundary condition. The figure also shows that the computed values of $\partial_z \psi_1^{(s)}(z = \infty, \beta, \omega_c)$ for small ω_c are in a good agreement with (3.18).

In summary, Eq. (3.18) shows that the tangential velocity away from the boundary asymptotes to a constant that is a function of β, and has a weak (logarithmic) dependence on the cut-off frequency ω_c. Therefore the asymptotic dependence in the stochastic case (with a cut-off) and the deterministic case is qualitatively similar, although the value of the asymptotic velocity of the former depends on β. Note also that this asymptotic behavior only sets in for distances larger than $(\nu/\omega_c \Omega)^{1/2}$, a value that can be quite large in practical microgravity conditions.

4. Randomly vibrating wavy boundary

In the two previous sections we considered cases in which the characteristic longitudinal length scale of the solid boundary was either infinite or large compared with the characteristic amplitude of boundary vibrations. We examine here the case of a wavy boundary and study how comparable length scales in both directions influence the flow away from the boundary. In contrast with the Schlichting problem, the external applied flow is now uniform or, alternatively, the length scale over which the flow is not uniform is much larger that the wavelength of the boundary. Thus one anticipates that the normal component of the flow that appears is caused by the wall profile. This flow interacts through nonlinear terms with the externally forced flow that is parallel to the average profile of the boundary and gives rise to stationary streaming. Even for stochastic vibration we show that positive and negative vorticity production in adjacent regions of the boundary introduces a natural decay length in the zeroth order solution, thus leading to exponential decay of the flow away from the boundary, even in the absence of a low frequency cut-off in the power spectrum of the boundary velocity.

Consider a rigid wavy wall being washed by a uniform oscillatory flow parallel to the wall wave vector,

$$\mathbf{u}(x, z = \infty) = (u_0(t), 0). \quad (4.1)$$

We now assume that $u_0(t)$ is a narrow band Gaussian process. Assume also that the amplitude of the boundary profile l is small compared with both the Stokes layer δ_s and the wavelength L, with δ_s/L finite. The following dimensionless quantities are introduced,

$$\left.\begin{array}{c} z = \tilde{z}[(\nu/\Omega)^{1/2}], \quad x = \tilde{x}[(\nu/\Omega)^{1/2}], \quad t = \tilde{t}[\Omega^{-1}], \quad \psi = \tilde{\psi}[(2\langle u_0^2\rangle \nu/\Omega)^{1/2}], \\[2mm] \epsilon = l/(\nu/\Omega)^{1/2}, \quad Re = \left[2\langle u_0^2\rangle/\Omega\nu\right]^{1/2}, \quad k = 2\pi(\nu/\Omega)^{1/2}/L, \quad \tilde{\Delta} = \partial_{\tilde{z}}^2 + \partial_{\tilde{x}}^2 \end{array}\right\}$$

$$(4.2)$$

referred to the Cartesian coordinate system sketched in Fig. 5. The solid boundary is located at

$$\tilde{\eta}(\tilde{x}) = \hat{\eta}\epsilon\exp(\mathrm{i}k\tilde{x}) + \text{c.c.} \tag{4.3}$$

with constant complex amplitude $\hat{\eta}$ so that $|\hat{\eta}| = 1/2$. The dimensionless (and two dimensional) Navier-Stokes equation (tildes are omitted in what follows) reads,

$$\partial_t\Delta\psi + Re\frac{\partial(\psi, \Delta\psi)}{\partial(z, x)} = \Delta^2\psi, \tag{4.4}$$

with no-slip conditions at the boundary,

$$\psi = 0, \quad \partial_z\psi = 0 \quad \text{at} \quad y = \eta(x), \tag{4.5a,b}$$

and the imposed uniform flow at infinity,

$$\partial_x\psi = 0, \quad \partial_z\psi = 2^{-1/2}u_0(t) \quad \text{at} \quad z = \infty. \tag{4.6a,b}$$

These equations depend only on three dimensionless parameters: ϵ, the ratio of the amplitude of the wavy wall to the boundary layer width; Re, the Reynolds number (the square root of Re_p used in Section 3); and k, the wavenumber of the wall profile in units of boundary layer width. We assume $\epsilon \ll 1$ and expand the stream function in a power series of ϵ,

$$\psi = \psi_0 + \epsilon\psi_1 + \ldots \tag{4.7}$$

The boundary conditions are likewise expanded in power series of ϵ,

$$\psi(z)|_{z=\eta} = \psi_0(z)|_{z=0} + \epsilon(\psi_1(z)|_{z=0} + \eta\partial_z\psi_0(z)|_{z=0}) + \ldots \tag{4.8}$$

We now solve (4.4) order by order in ϵ.

At zeroth order the wall is effectively planar. We decompose the Fourier transform of the stream function as, $\hat{\psi}_0(x, z, \omega) = 2^{-1/2}\hat{u}_0(\omega)\hat{\zeta}_0(z, \omega)$. The function $\hat{\zeta}_0(z, \omega)$ is given in Eq. (3.10). At this order, the solution is identical to that found for a planar boundary.

At first order we seek a solution of the form,

$$\psi_1 = \hat{\eta}\exp(\mathrm{i}kx)\phi(z, t) + \text{c.c.} \tag{4.9}$$

so that the amplitude $\phi(z, t)$ satisfies the Orr-Sommerfeld equation,

$$(\partial_t\mathcal{D} - \mathcal{D}^2)\phi = \mathrm{i}kRe(\partial_z^3\psi_0 - \partial_z\psi_0\mathcal{D})\phi, \quad \mathcal{D} = \partial_z^2 - k^2 \tag{4.10}$$

with non-homogeneous boundary conditions,

$$\phi = 0, \quad \partial_z\phi = -\partial_z^2\psi_0 \quad \text{at} \quad z = 0, \tag{4.11a,b}$$

$$\phi = 0, \quad \partial_z\phi = 0 \quad \text{at} \quad z = \infty, \tag{4.12a,b}$$

The linear operator in the left hand side of Eq. (4.10) contains a significant difference with respect to that of Eq. (3.11), the equation governing the first order stream function

for the case of a slightly curved boundary. Both equations describe vorticity diffusion, but the biharmonic equation (4.10) contains a cut-off through the parameter k. Is is precisely this term that will lead to an asymptotic exponential decay of the velocity field sufficiently far away from the boundary for any finite β. The exponential decay at long distances arises from the screening introduced by the simultaneous positive and negative vorticity produced at the troughs and crests of the wavy wall.

In order to obtain a solution of the Orr-Sommerfeld equation (Eq. (4.10)), we further expand the amplitude $\phi(z,t)$ in power series of $kRe = 2\pi \left(2 \langle u_0^2 \rangle \right)^{1/2} /L\Omega$. This is the ratio between the amplitude of oscillation of the flow at infinity and the wall wavelength. We write,

$$\phi = \phi_0 + ikRe\phi_1 + \dots \tag{4.13}$$

The function ϕ_0 obeys the linearized Eq. (4.10) with boundary conditions as in Eqs. (4.11-4.12) with ϕ replaced by ϕ_0. The Fourier transform of ϕ_0 is given by,

$$\hat{\phi}_0(z,\omega) = (2)^{-1/2}\hat{u}_0(\omega)\frac{\alpha}{\rho - k} \left(e^{-\rho z} - e^{-kz}\right), \tag{4.14}$$

with $\rho \equiv (\alpha^2 + k^2)^{1/2}$, and the principal branch of the square root is assumed ($\Re\{\rho\} > 0$). Recall that $\alpha = (1 + i\mathrm{sign}(\omega))(\omega/2\nu)^{1/2}$. The field ϕ_0 describes vorticity diffusion near the wavy wall caused by the uniform but oscillatory far field flow. Both the spatial and ensemble averages of this flow are zero. However, the flow non-uniformity at this order induces mean flow at the next order, as it is readily apparent from the equation for ϕ_1,

$$(\partial_t \mathcal{D} - \mathcal{D}^2)\phi_1 = (\partial_z^3 \psi_0 - \partial_z \psi_0 \mathcal{D})\phi_0, \tag{4.15}$$

with boundary conditions $\phi_1 = 0$, $\partial_z\phi_1 = 0$ at $z = 0, \infty$. The field ϕ_1 describes vorticity diffusion forced by the nonlinear interaction between ϕ_0 and ψ_0. As was the case in Sec. 3, we focus on the long time limit of the ensemble average of Eq. (4.15) $\phi_1^{(s)} = \lim_{t\to\infty} \langle\phi_1\rangle = \chi + \text{c.c.}$, where χ is given by,

$$\mathcal{D}^2\chi = -\frac{1}{2}G(z,\beta), \tag{4.16}$$

with,

$$G(z,\beta) = \int_0^\infty d\omega\, P(\omega,\beta)\, Q(z,\omega,\beta),$$

$$Q(z,\omega,\beta) = \alpha(\rho + k)(2e^{-(\alpha^*+\rho)z} - e^{-(\alpha^*+k)z} - e^{-\rho z}). \tag{4.17}$$

The corresponding boundary conditions are homogeneous, $\chi = 0$, $\partial_z\chi = 0$ at $z = 0, \infty$. The solution is,

$$\chi(z,\beta) = \int_0^\infty d\omega\, P(\omega,\beta)\hat{\chi}(z,\omega),$$

$$\hat{\chi}(z,\omega) = A_1 e^{-\rho z} + A_2 e^{-(\alpha^*+\rho)z} + A_3 e^{-(\alpha^*+k)z} + (B_1 + zB_2)e^{-kz} \tag{4.18}$$

where the functions A_i, B_i depend on frequency and wavenumber,

$$A_1 = D/\alpha^4, \quad A_2 = D/(2\alpha^2\rho^2), \quad A_3 = -D/(\alpha^2(\alpha^* + 2k)^2), \quad D = \alpha(\rho + k)/2,$$
$$B_1 = -(A_1 + A_2 + A_3), \quad B_2 = (\rho - k)A_1 + (\rho + \alpha^* - k)A_2 + \alpha^* A_3. \tag{4.19}$$

Therefore the stationary part of the averaged first order stream function is given by,

$$\psi_1^{(s)} = ikRe\hat{\eta}\exp(ikx)(\chi + \chi^*) + \text{c.c.} \tag{4.20}$$

This solution shows that $\psi_1^{(s)}$ has a phase advance of $\pi/2$ with respect to the wall profile, and hence the flow in the vicinity of the boundary is directed from trough to crest $(\partial_z^2(\chi + \chi^*)|_{z=0} > 0)$. By shifting the coordinate system along the x axis we can change the phase of the wall profile so as to make it a simple cosine function. We consider $\eta(x) = \epsilon\cos(kx)$ in what follows.

Following Lyne (1971), we now proceed to study the limits of k large and small, while $kRe \ll 1$. For $k \gg 1$ the wavelength of the boundary profile is much smaller that the thickness of the viscous layer. In this case, a boundary layer appears of characteristic thickness $1/k$. Screening between regions producing positive and negative vorticity occurs over a distance much smaller that the Stokes thickness based on the frequency of oscillation. The net vorticity does not diffuse even to distances of order $z \sim \mathcal{O}(1)$, hence giving rise to exponential decay with an $\exp(-kz)$ factor. The region in which the stream function is not exponentially small depends on $Z = kz$. The explicit form of $\psi_1^{(s)}$ may be obtained by direct expansion of the solution (4.20) in power series of $1/k$, keeping Z fixed. The leading contribution to the steady part of the tangential component of the velocity is given by,

$$u_1^{(s)} = k\partial_Z\psi_1^{(s)} \sim -\frac{Re}{24k^2}\sin(kx)\,\mathrm{e}^{-Z}Z(6 - Z^2) \qquad (4.21)$$

The boundary layer comprises two recirculating cells per wall period, located within $0 < z \lesssim 1/k$. The separation point is given by $z^2 = 6/k^2$.

In the opposite limit of $k \ll 1$ one formally recovers the Schlichting problem in that the characteristic longitudinal length scale is much larger than the Stokes layer thickness. There is one fundamental difference, however, which can be seen from the solution, Eq. (4.18). It has two contributions: the first one is proportional A_i, arises from the particular solution,and serves to balance the non-homogeneity in Eq. (4.16). This contribution decays within the Stokes layer. The second one is proportional to B_i, and arises from the general solution of the homogeneous part of the equation. This contribution decays over the stretched scale Z. It turns out that this second contribution introduces an additional separation of the composite boundary layer when $0 < k \leqslant 0.23$. The lines of zero value of the longitudinal component of the steady velocity profile are shown Fig. 6. The location of the second separation point is entirely determined by that part of the solution that is proportional to B_i, and occurs at $z \sim \mathcal{O}(1/k) \gg 1$.

The steady velocity may be obtained by expanding the exact solution (Eq. (4.18)) in power series of k, first keeping z fixed (inner solution, $u_{1i}^{(s)}$), and second keeping Z fixed (outer solution $u_{1o}^{(s)}$). To leading order, we find,

$$u_{1i}^{(s)}(z') \sim -Rek^2\sin(kx)\left\{\left[\frac{z'}{2}(\sin(z') - \cos(z')) + 2\sin(z') + \frac{1}{2}\cos(z')\right]\mathrm{e}^{-z'}\right.$$

$$\left. + \frac{\mathrm{e}^{-2z'}}{4} - \frac{3}{4}\right\}, \quad z' = z/2^{1/2} \sim \mathcal{O}(1), \qquad (4.22)$$

$$u_{1o}^{(s)}(Z) \sim -Rek^2\sin(kx)\left[\frac{3}{4}(Z - 1)\mathrm{e}^{-Z}\right], \qquad Z \sim \mathcal{O}(1). \qquad (4.23)$$

The solution for the inner and outer steady velocities was already obtained by Lyne (1971) by a conformal transformation technique. We further note that the inner and outer solutions can now be matched by requiring that $u_{1i}^{(s)}(\infty) = u_{1o}^{(s)}(0) = 3/4Rek^2\sin(kx)$. Hence it is possible to construct a uniformly valid solution by adding the inner and outer solutions, and subtracting the first term of the inner expansion of the outer solution. We

find,

$$u_{1c}^{(s)}(z') \sim -Rek^2\sin(kx)\left\{\left[\frac{z'}{2}(\sin(z') - \cos(z')) + 2\sin(z') + \frac{1}{2}\cos(z')\right]\mathrm{e}^{-z'}\right.$$

$$\left. + \frac{\mathrm{e}^{-2z'}}{4} + \frac{3}{4}(2^{1/2}kz' - 1)\mathrm{e}^{-2^{1/2}kz'}\right\} \tag{4.24}$$

We now turn to a numerical study of the case of finite β. The boundary value problem (4.16) has been solved numerically by using a multiple shooting method for non stiff and linear boundary value problems (Mattheij & Staarink (1984)). The method has the advantage that the necessary intermediate shooting points are determined by the method itself, and that it can give the solution on a preset and nonuniform grid of points. The code was tested on the analytically known solution of the deterministic limit, Eqs. (4.18) and (4.19). Our results are summarized in Figs. 6, 7 and 8.

Figure 6 shows the separation points of the stationary velocity as a function of the boundary wavenumber k for a range of values of β, including for reference the deterministic limit of $\beta = \infty$ (separation points are defined to be the zeros of the stationary tangential velocity). This figure shows that for fixed k, the mean stationary velocity field may be comprised of two or four recirculating cells per wall period depending on β. The first separation point is largely independent of β, whereas the deviation of the second relative to its value in the monochromatic limit is proportional to $\beta/\pi(1 + \beta^2)$, the value of $P(0, \beta)$.

Our results in the limit $k \ll 1$ are presented in Fig. 7, where profiles of tangential component of the mean stationary velocity are plotted for $k = 0.1$ and different values of β. At large β (close to the monochromatic limit) the flow is comprised of four recirculating cells per boundary period. Upon decresing β, the second separation point moves to infinity (see also Fig. 6), so that beyond some critical value of β, only two recirculating cells remain. Further decrease in β results in the reappearance of the second separation point at infinity, which then continues to move towards decreasing z. The intensity of the recirculating modes does not change monotonically with β as we further discuss below. In the opposite limit of $k \gg 1$ (Fig. 8 shows the case $k = 10.0$; note that $u_1^{(s)}$ is now normalized by Re/k^2), the qualitative structure of the flow is largely independent of β. The streaming flow has two recirculating cells per wall wavelength, and their intensity increases monotonically with decreasing β.

The complex dependence of the flow on β and k can be qualitatively understood from the interplay between the width of the power spectrum (given by $1/\beta$), the viscous damping of each elementary excitation that depends on its frequency, and the penetration depth of the flow field which is primarily dictated by the boundary wavelength. For small k, large frequency modes are damped close to the boundary and do not penetrate much into the recirculating layers. Reducing β introduces high frequency components into the driving terms at first order, but they are dynamically damped. At the same time, the power in the dominant frequency components (around Ω) decreases. Overall, a decrease in β then leads to a decrease in recirculation strength. As k increases, larger frequencies contribute to the flow over the entire range of the recirculating cells. Decreasing β decreases the strength of the dominant components, but increases the range of high frequencies that can contribute to the flow. From Eq. (4.16) one can show that the driving contribution from higher frequencies which is contained in Q increases faster with frequency than the decreasing weight given to them by the power spectrum $P(\omega, \beta)$. Consequently, decreasing β (which amounts to moving towards the white noise limit) leads to increasing amplitude of the recirculation.

In summary, for any value of β, finite or infinite, the vorticity produced by vibration of the wavy boundary does not penetrate into the bulk farther than a distance of order of the wavelength of the boundary. However, there are qualitative differences with the deterministic limit in the character of the flow within that layer. In particular, the structure and the intensity of the stationary secondary flow strongly depend on β.

5. Summary

We have addressed the flow induced by a randomly vibrating solid boundary in an otherwise quiescent fluid. This analysis has been motivated by the random residual acceleration field in which microgravity experiments are conducted. The salient features of the flow are summarized below.

When the solid boundary is planar, the flow field averages to zero (the average velocity of the boundary has been taken to be zero in all cases investigated), but its variance decays algebraically with distance away from the wall. This dependence follows from a non vanishing power spectrum of the boundary velocity at zero frequency. Introducing a low frequency cut-off in the power spectrum leads back to the classical exponential decay, with a rate that is determined by the cut-off frequency, Eq. (2.27). The amplitude of the decaying variance depends explicitly on the correlation time of the boundary velocity, $\beta = \Omega\tau$, where Ω is the dominant angular frequency of the power spectrum of the boundary velocity, and τ is inverse spectral width (τ is the correlation time of the boundary velocity).

If the solid boundary is curved, steady streaming is generated in analogy with the classical analysis of Schlichting. The stationary part of the ensemble average of the secondary velocity is nonzero, even though the boundary velocity averages to zero. In this case, we find that the leading contribution to the average stationary velocity diverges logarithmically with distance away from the boundary. In analogy to the planar case, the introduction of a low frequency cut-off in the power spectrum of the boundary velocity changes the asymptotic behavior qualitatively. The average stationary velocity asymptotes now to a constant, given by Eq. (3.18). The asymptotic velocity explicitly depends on β and logarithmically on the cut-off frequency. This asymptotic behavior is not reached until a length scale of the order of the Stokes layer thickness that is based on the cut-off frequency.

We have finally analyzed the case of a periodically modulated solid boundary in the limit in which the scale of the wall modulation is small compared to the thickness of the Stokes layer, and also when the spatial amplitude of the boundary oscillation is small compared with the wavelength of the wall profile. Cancellation of vorticity production over the wall boundary leads to exponential decay of the fluid velocity away from the boundary, with a decay length which is proportional to the wall wavelength, even if the zero frequency value of the power spectrum of the boundary velocity is nonzero. If the boundary wavelength is much larger than the Stokes layer thickness, we find steady streaming in secondary flow with two or four recirculating cells per wall period depending on β. On the other hand, if the wavelength is much smaller than the Stokes layer thickness, only two recirculating cells are formed regardless of the value of β. Somewhat unexpectedly, the intensity of the recirculation can both increase or decrease with β.

REFERENCES

ALEXANDER, J.I.D. 1990 Low-gravity experiment sensitivity to residual acceleration: a review. *Microgravity sci. technol.* **3**, 52.

ALEXANDER, J.I.D., GARANDET, J.P., FAVIER, J.J. & LIZEE, A. 1997 g-jitter effects on segregation during directional solidification of tin-bismuth in the mephisto furnace facility. *J. Crystal Growth* **178**, 657.

ALEXANDER, J.I.D., OUAZZANI, J. & ROSENBERGER, F. 1991 Analysis of the low gravity tolerance of Bridgman-Stockbarger crystal growth. *J. Crystal Growth* **113**, 21.

BATCHELOR, G.K. 1967 *An Introduction to Fluid Dynamics*. Cambridge: Cambridge University Press.

BLONDEAUX, P. & VITTORI, G. 1994 Wall imperfections as a triggering mechanism for Stokes layer transition. *J. Fluid Mech.* **264**, 107.

CARSLAW, H.S. & JAEGER, J.C. 1959 *Conduction of heat in solids*. Oxford: Clarendon Press.

DELOMBARD, R., MCPHERSON, K., MOSKOWITZ, M. & HROVAT, K. 1997 Comparison tools for assessing the microgravity environment of missions, carriers and conditions. *Tech. Rep.* TM 107446. NASA.

FAROOQ, A. & HOMSY, G.M. 1994 Streaming flows due to g-jitter-induced natural convection. *J. Fluid Mech.* **271**, 351.

GERSHUNI, G.Z. & LYUBIMOV, D.V. 1998 *Thermal Vibrational Convection*. New York: John Wiley & Sons.

GERSHUNI, G.Z. & ZHUKHOVITSKII, E.M. 1976 *Convective Stability of Incompressible Fluids*. Jerusalem: Keter.

GRADSHTEYN, I.S. & RYZHIK, I.M. 1980 *Tables of integrals, series and products*. New York: Academic Press.

GRASSIA, P. & HOMSY, G.M. 1998a Thermocapillary and buoyant flows with low frequency jitter. I. jitter confined to the plane. *Phys. Fluids* **10**, 1273.

GRASSIA, P. & HOMSY, G.M. 1998b Thermocapillary and buoyant flows with low frequency jitter. II. spanwise jitter. *Phys. Fluids* **10**, 1291.

KAMOTANI, Y., PRASAD, A. & OSTRACH, S. 1981 Thermal convection in an enclosure due to vibrations aboard a spacecraft. *AIAA J.* **19**, 511.

KANEKO, A. & HONJII, H. 1979 Double structures of steady streaming in the oscillatory viscous flow over a wavy wall. *J. Fluid Mech.* **93**, 727.

LYNE, W.H. 1971 Unsteady viscous flow over a wavy wall. *J. Fluid Mech.* **50**, 33.

MATTHEIJ, R.M.M. & STAARINK, G.W.M. 1984 An efficient algorithm for solving general linear two-point bvp. *SIAM J. Sci. Stat. Comp.* **5**, 745.

NAYFEH, A.H. 1981 *Introduction to Perturbation techniques*. New York: John Wiley & Sons.

NELSON, E.S. 1991 An examination of anticipated g-jitter on space station and its effects on materials processes. *Tech. Rep.* TM 103775. NASA.

SCHLICHTING, H. 1979 *Boundary layer theory*, 7th edn. New York: McGraw-Hill.

STOKES, G.G. 1851 *Trans. Camb. Phil. Soc.* **9**, 8, Mathematical and Physical Papers **3**,1.

STRATONOVICH, R.L. 1967 *Topics in the Theory of Random Noise*, vol. II. New York: Gordon and Breach.

THOMSON, J.R., CASADEMUNT, J., DROLET, F. & VIÑALS, J. 1997 Coarsening of solid-liquid mixtures in a random acceleration field. *Phys. Fluids* **9**, 1336.

VAN DYKE, M. 1964 *Perturbation Methods in Fluid Mechanics*. New York: Academic Press.

VITTORI, G. 1989 Non-linear viscous oscillatory flow over a small amplitude wavy wall *J. Hydr. Res.* **27**, 267.

WALTER, H.U., ed. 1987 *Fluid Sciences and Materials Sciences in Space*. New York: Springer Verlag.

ZHANG, W., CASADEMUNT, J. & VIÑALS, J. 1993 Study of the parametric oscillator driven by narrow band noise to model the response of a fluid surface to time-dependent accelerations. *Phys. Fluids A* **5**, 3147.
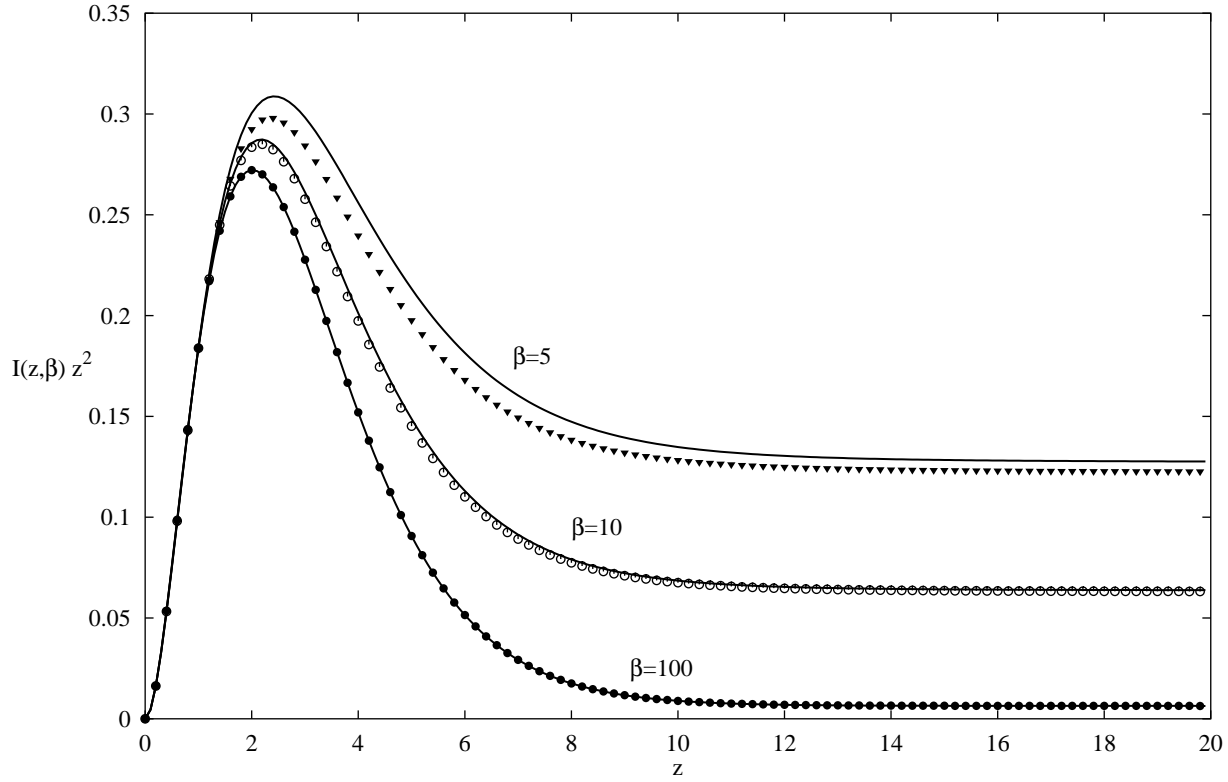
FIGURE 1. Normalized variance of the tangential velocity for the case of a planar boundary computed by numerical integration of Eq. (2.21) (symbols), and its uniform asymptotic expansion, Eq. (2.23), (solid lines). The function $I(z, \beta) z^2$ asymptotes to a constant value outside of the classical Sokes layer based on Ω. The uniform expansion remains a good approximation even for moderate β.
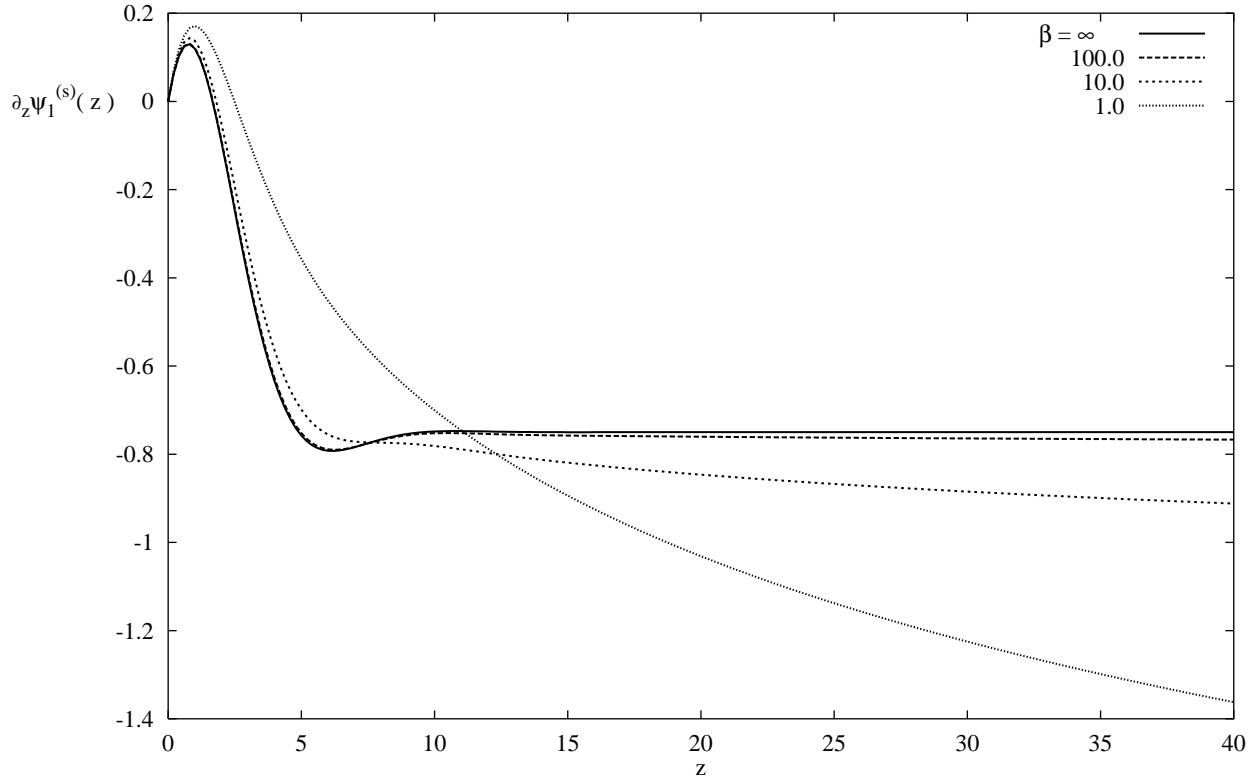
FIGURE 2. Stationary first order velocity as a function of distance for a range of values of β. All curves diverge logarithmically at large z, except for $\beta = \infty$ (monochromatic limit), in which the velocity asymptotes to a constant within the Stokes layer. This latter behavior reproduces the classical result of Schlichting.
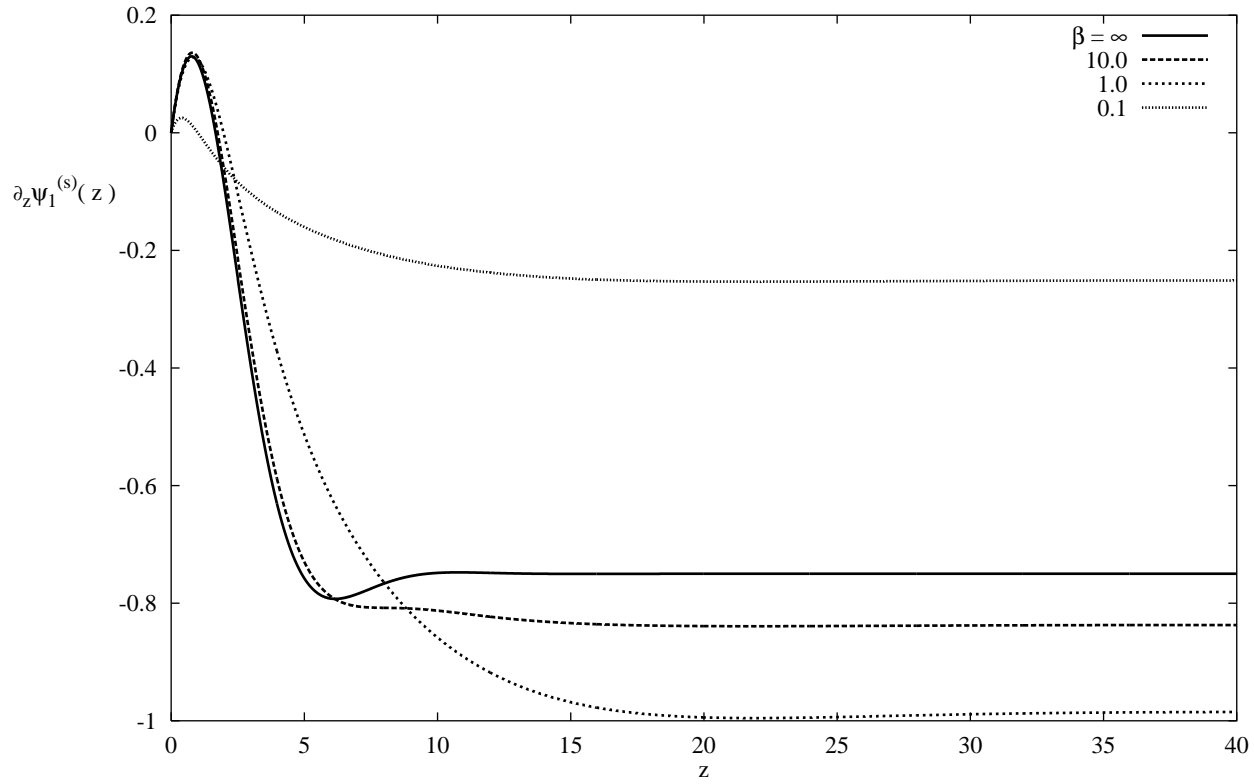
FIGURE 3. Stationary first order velocity as a function of distance for a range of values of β. The power spectrum of the boundary velocity has a low frequency cut-off at $\omega_c = 0.05$. The velocity asymptotes to a constant that depends on the value of β.
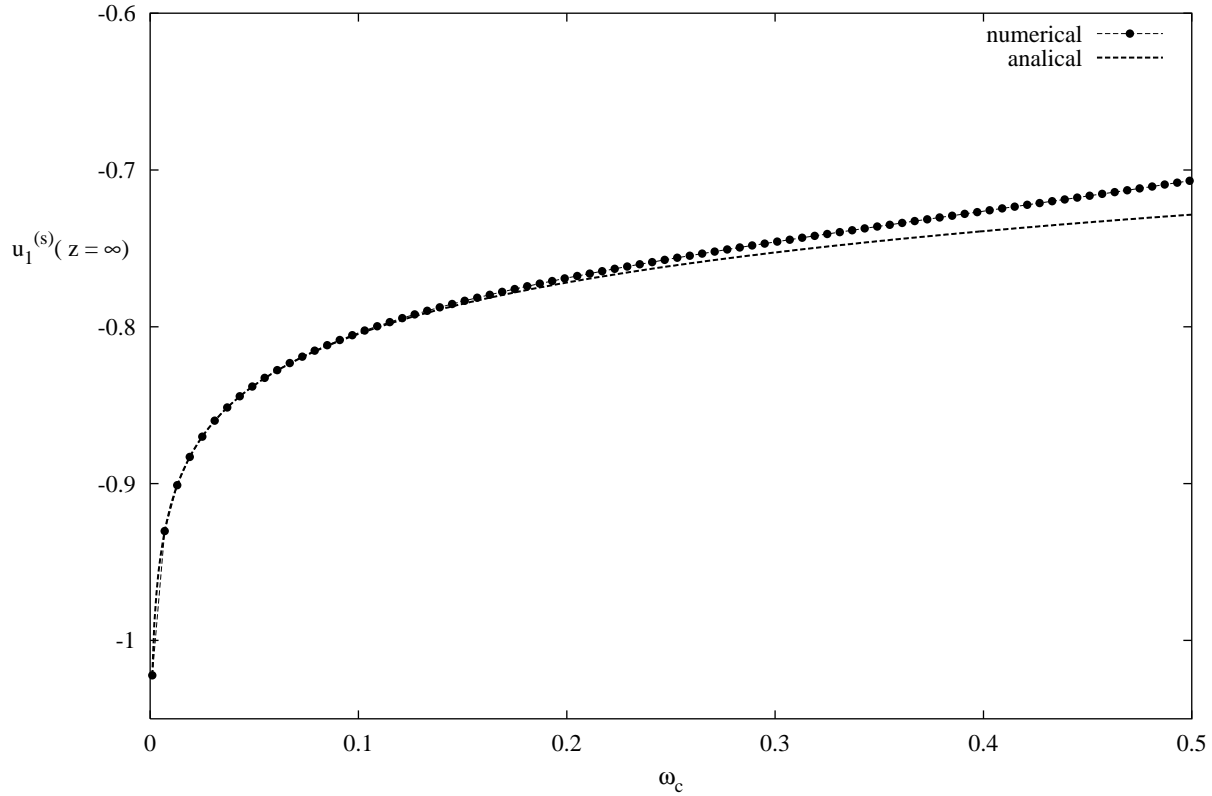
FIGURE 4. Asymptotic dependence of the stationary velocity as a function of the cut-off frequency ω_c. We show the case $\beta = 10$ given by Eq. (3.18) along with the numerically obtained solution.
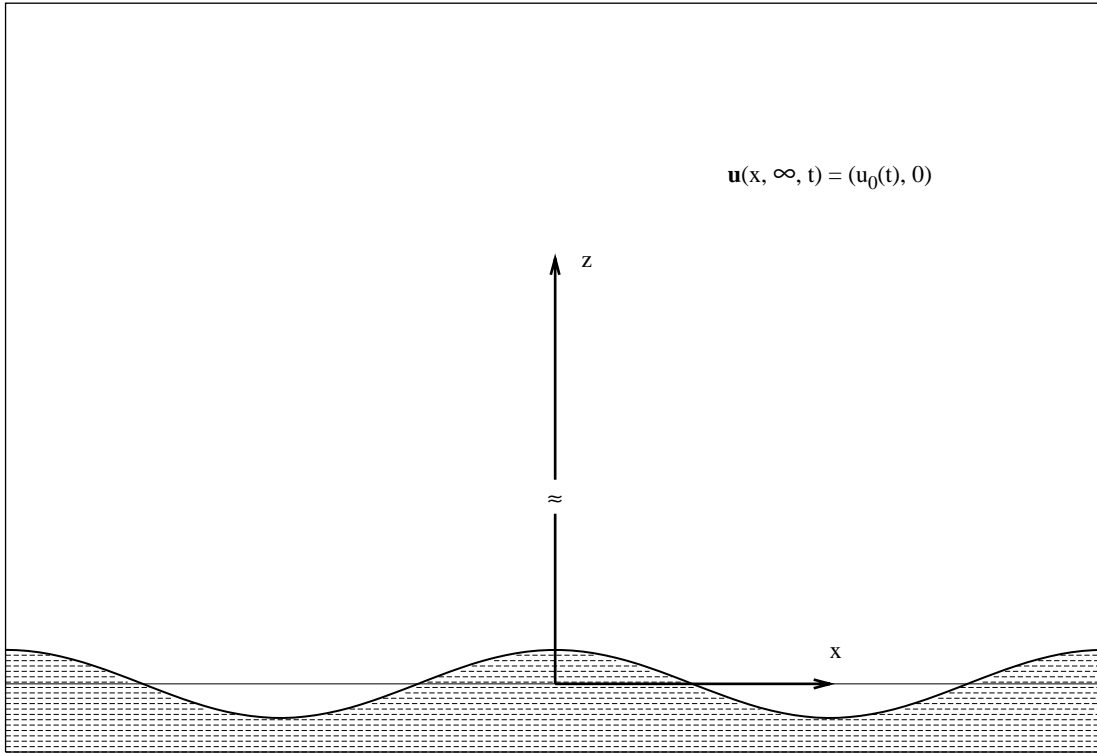
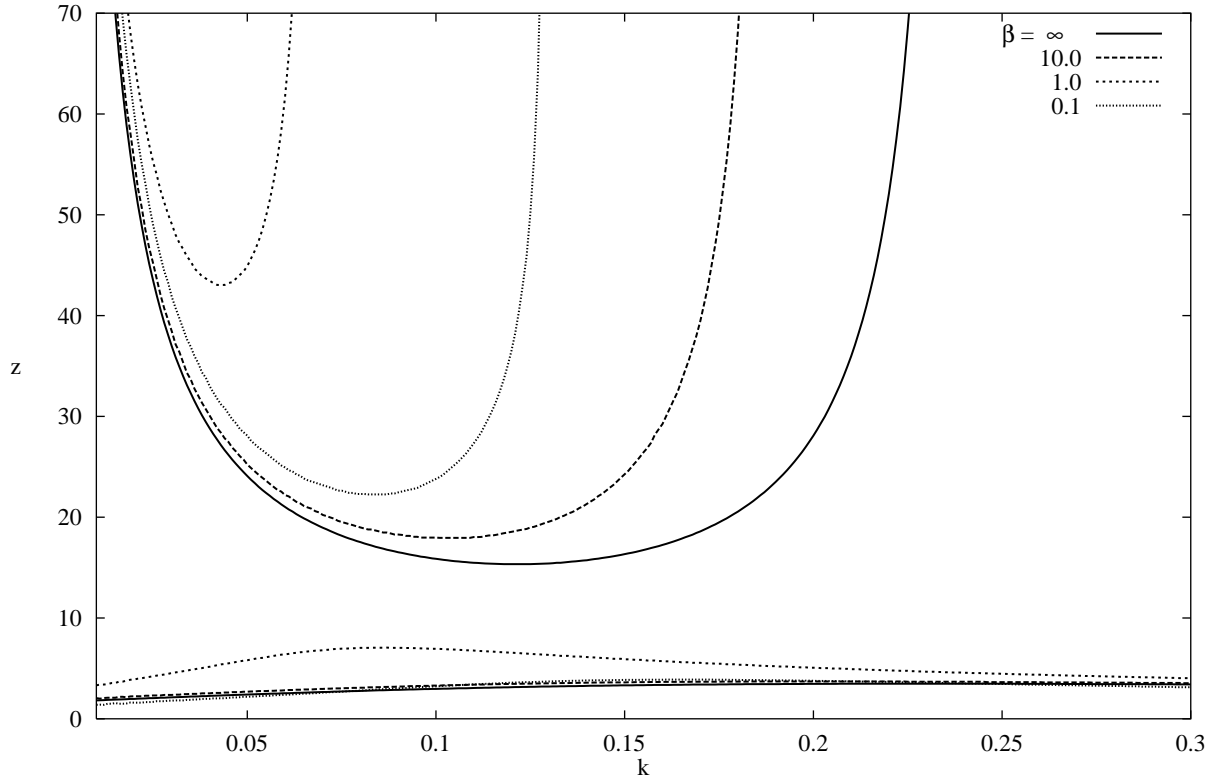FIGURE 5. Schematic view of the geometry of the wavy wall studied in Section 4.

FIGURE 6. Separation points of the boundary layer over the wavy boundary as a function of its wavenumber k, for different values of β. The separation points are the loci of zero tangential velocity. At fixed k, the location of the second separation point depends strongly on β.
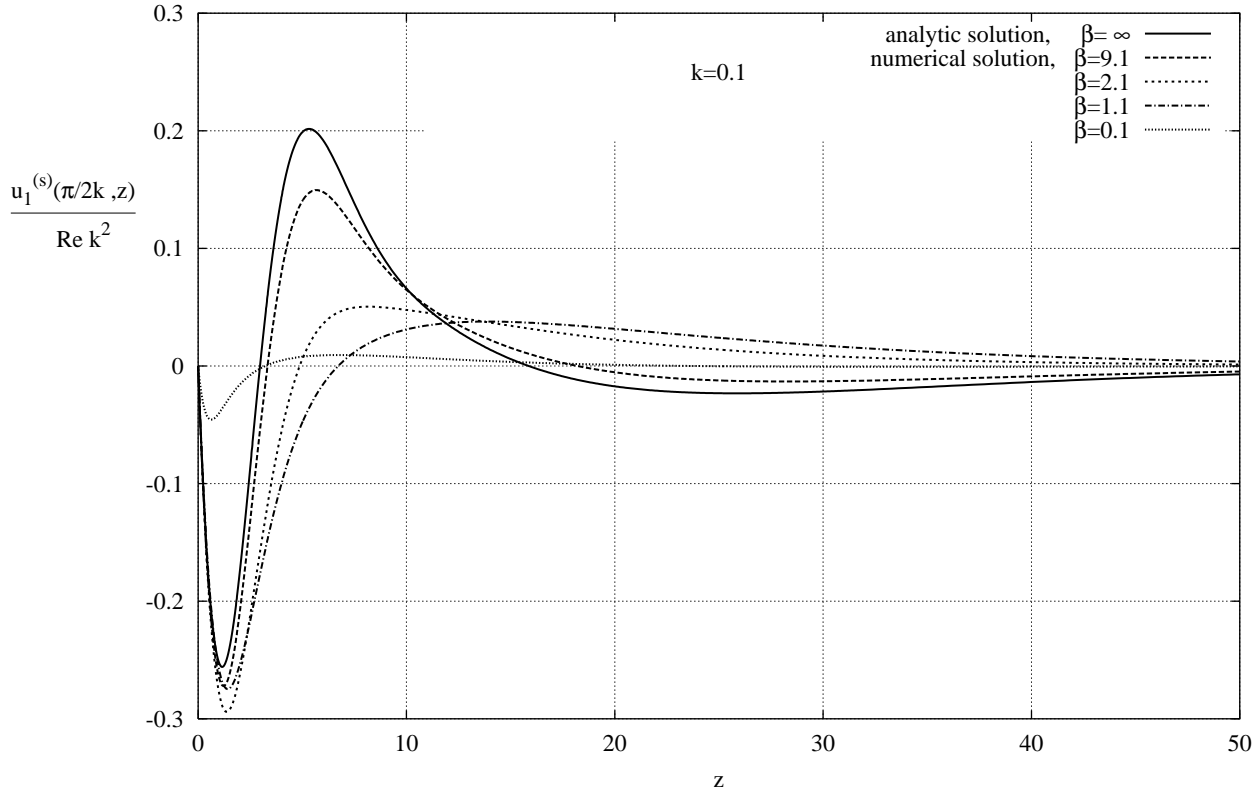
FIGURE 7. Tangential component of the mean stationary velocity as a function of z for $k = 0.1$ and a range of values of β. The case $\beta = \infty$ corresponds to analytic solution obtained by Lyne. The other curves are the numerical solutions of the boundary value problem defined by Eq. (4.16) and corresponding boundary conditions.
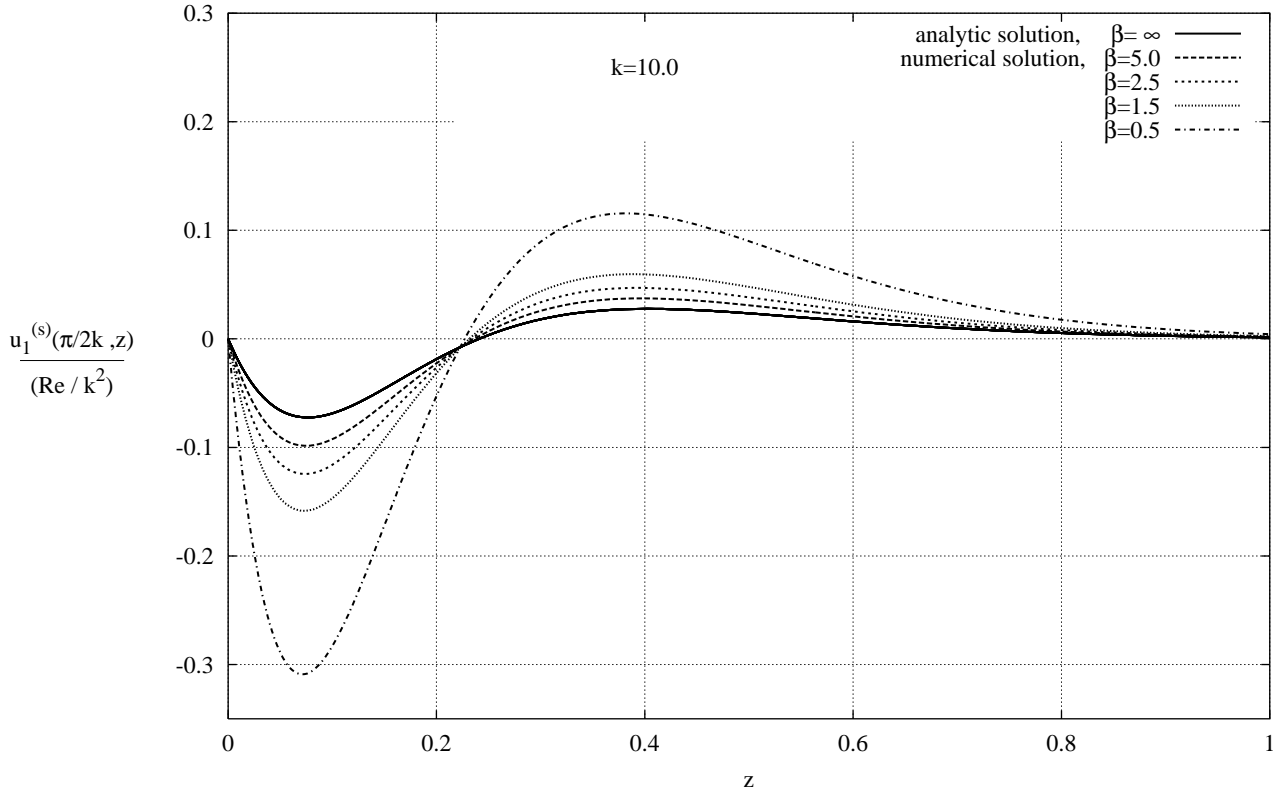
FIGURE 8. Tangential component of mean stationary velocity as a function of z for $k = 10$ and a range of values of β. The case $\beta = \infty$ corresponds to analytic solution obtained by Lyne. The other curves are the numerical solutions of the boundary value problem defined by Eq. (4.16) and corresponding boundary conditions.